



A Journal of the Gesellschaft Deutscher Chemiker

# Angewandte Chemie

GDCh

International Edition

www.angewandte.org

## Accepted Article

**Title:** Gas-Phase Ion Fluorescence Spectroscopy of Tailor-made Rhodamine Homo- and Heterodyads: Quenching of Electronic Communication by  $\pi$ -Conjugated Linkers

**Authors:** Steen Brøndsted Nielsen, Anne Ugleholdt Petersen, Christina Kjær, Cecilie Jensen, and Mogens Brøndsted Nielsen

This manuscript has been accepted after peer review and appears as an Accepted Article online prior to editing, proofing, and formal publication of the final Version of Record (VoR). This work is currently citable by using the Digital Object Identifier (DOI) given below. The VoR will be published online in Early View as soon as possible and may be different to this Accepted Article as a result of editing. Readers should obtain the VoR from the journal website shown below when it is published to ensure accuracy of information. The authors are responsible for the content of this Accepted Article.

**To be cited as:** *Angew. Chem. Int. Ed.* 10.1002/anie.202008314

**Link to VoR:** <https://doi.org/10.1002/anie.202008314>

## RESEARCH ARTICLE

# Gas-Phase Ion Fluorescence Spectroscopy of Tailor-made Rhodamine Homo- and Heterodimers: Quenching of Electronic Communication by $\pi$ -Conjugated Linkers

Anne Ugleholdt Petersen,<sup>[a]</sup> Christina Kjær,<sup>[b]</sup> Cecilie Jensen,<sup>[a]</sup> Mogens Brøndsted Nielsen,<sup>\*[a]</sup> and Steen Brøndsted Nielsen<sup>\*[b]</sup>

[a] Dr. A. U. Petersen, C. Jensen, Prof. Dr. M. Brøndsted Nielsen  
Department of Chemistry  
University of Copenhagen  
E-mail: mbn@chem.ku.dk

[b] Dr. C. Kjær, Prof. Dr. S. Brøndsted Nielsen  
Department of Physics and Astronomy  
Aarhus University  
E-mail: sbn@phys.au.dk

Supporting information for this article is given via a link at the end of the document.

**Abstract:** While many key photophysical features are understood for electronic communication between chromophores in neutral compounds, there is limited information on the effect of charges in practically relevant ionic chromo/fluorophores. Here we have chosen positively charged rhodamines and prepared a selection of homo- and heterodimers with alkyl or  $\pi$ -conjugated, acetylenic bridges. Protonated molecules were transferred as isolated ions to gas phase where there is no solvent screening of charges, and fluorescence spectra were measured with a custom-made ion-trap setup. Our work reveals strong polarization of the  $\pi$ -spacer (induced dipole/quadrupole) when it experiences the electric field from one / two dyes. Hence,  $\pi$ -spacers provide efficient shielding of charges by reducing the Coulomb interaction, whereas two dye cations polarize each other when connected by an alkyl. The screening influences the Förster Resonance Energy Transfer efficiency that relies on the dipole-dipole interaction.

## Introduction

The photophysics of many biological systems is governed by electronic interactions between two or more chromophores (light absorbers). One important example is photosynthesis where multiple chlorophyll molecules within photosynthetic proteins are responsible for light harvesting and efficient energy transfer to the reaction center where charge separation occurs.<sup>[1]</sup> Another is the nontrivial quantum physics of stacked bases in DNA and Watson-Crick base pairs, which determines the excited-state dynamics and fate after UV excitation.<sup>[2]</sup>

When two chromophores are in close proximity, exciton coupling of the two individual excited-state wavefunctions occurs, which implies that the new stationary states are not associated with only one of the chromophores but with both; in other words, the excitation energy is spatially delocalized over both chromophores.<sup>[3]</sup> At large separations the coupling is weak, and we can to a good approximation consider the excitation being associated with only one chromophore. Förster Resonance Energy Transfer (FRET) is then responsible for a downhill movement of the excitation energy between chromophores

situated in a network.<sup>[4]</sup> The efficiency of energy transfer strongly depends on the separation between two chromophores and is inversely proportional to the power of six. At the so-called Förster distance  $R_0$ , the efficiency is 50%. Two important factors that determine  $R_0$  are the reorientation factor and the spectral overlap of the donor-emission spectrum and the acceptor-absorption spectrum. The former depends on the orientation of the two transition-dipole moments relative to each other and to the interfluorophore distance vector.

In most textbooks the interaction between two chromophores (or fluorophores) is typically described with the assumption that both chromophores are neutral, and that they do not perturb each other in the ground state (see e.g., [3]). Indeed, the two examples mentioned above involve neutral chlorophylls and DNA bases where such assumptions are reasonable. However, many dyes used as labels in FRET experiments on biomacromolecules are ionic, e.g., positively charged rhodamine and cyanine dyes and negatively charged fluorescein ones.<sup>[4]</sup> One ionic dye provides an electric field at the other dye when the two are in close proximity, which causes an induced dipole moment and *vice versa*. Hence two, say, cationic dyes actually communicate in the ground state even though there is no overlap of their electronic wavefunctions. Photoexcitation of one dye increases its polarizability and as a result leads to an increase in the average distance between the positive charge distributions of the two dyes. The resultant Stark shift of energy levels is evidenced from redshifted emission spectra as reported in previous gas-phase work on homodimers of rhodamine 575 cations (**R575<sup>+</sup>**)<sup>[5]</sup> and heterodimers of **R575<sup>+</sup>** and rhodamine 640 cations (**R640<sup>+</sup>**)<sup>[6]</sup>; the two dyes were bridged by either methylene linkers or peptides.

It is clear that the internal Coulomb repulsion is largest when the dyad systems are isolated *in vacuo* where there is no solvent screening of the two charges. Gas-phase experiments on simple model systems therefore provide the most direct information on such charge-charge interactions. Unfortunately, however, such experiments suffer from a thin cloud (low density) of ionic fluorophores, and specialized apparatus is needed to obtain reasonable signal-to-noise ratios.<sup>[7]</sup>

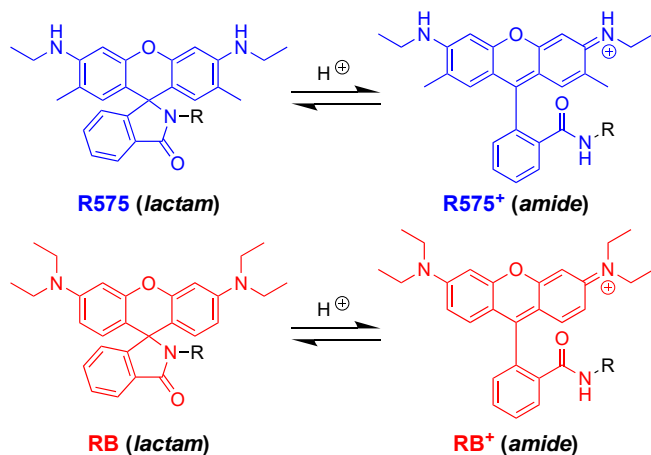
## RESEARCH ARTICLE

In Aarhus we use the home-built LUNA (LUMinescence iNstrument in Aarhus) setup where ions produced by electrospray ionization are stored in the center of a cylindrical Paul trap.<sup>[8]</sup> Mass selection is followed by photoexcitation and collection of emitted photons. One of the end electrodes is a mesh grid to allow as many photons as possible to exit the trap and be detected. The photon collection efficiency of our setup is about 5%. While one obvious requirement for gas-phase ion fluorescence spectroscopy is that the ions are fluorescent, the technique benefits from no limitation on the size of the molecular ion. This is in contrast to photodissociation-action spectroscopy where dissociation on the instrumental time scale is necessary, *i.e.*, microseconds to tens of milliseconds dependent on the setup used, and dissociation yields can significantly depend on excitation wavelengths.<sup>[9]</sup>

In this work we have synthesized a multitude of homo- and heterodimers of rhodamine 575 (**R575**) and rhodamine B (**RB**) connected by alkyl or  $\pi$ -conjugated, linear bridges that represent new unexplored dyad systems. Our synthesis work is based on development of suitable acetylenic building blocks that were subjected to metal-catalyzed coupling reactions under various conditions. The compounds isolated are on the closed lactam forms (**R575** / **RB**) but upon protonation, they undergo ring-opening to form the cationic and fluorescent amide forms (**R575<sup>+</sup>** / **RB<sup>+</sup>**) as shown in Scheme 1. In heterodimers, **R575<sup>+</sup>** is the donor and **RB<sup>+</sup>** the acceptor. The  $\pi$ -spacer is linked to the lactam/amide nitrogen atom of the dye via a methylene group and is therefore not in conjugation with the chromophore unit.

A summary of ions that were subjected to gas-phase fluorescence experiments is given in Figure 1; these include also relevant monomer derivatives for comparison. Our results reveal differences in the communication between two ionic dyes with the nature of the linker, and that a  $\pi$ -linker may to some extent act as an electrostatic shield between the two dyes.

It should be noted that photoexcited electron transfer from one dye to another, often mediated by a  $\pi$ -conjugated bridge,<sup>[10]</sup> is not energetically feasible for our gas-phase dyads as the detachment energy of a cationic donor is too high compared with the recombination energy of the cationic acceptor (energy defect of about 6 eV<sup>[6]</sup>). The only possible processes after photoexcitation are therefore light emission from either **R575<sup>+</sup>** or **RB<sup>+</sup>**, potentially after FRET in the latter case.



Scheme 1. Equilibria between closed and open, protonated rhodamine forms.

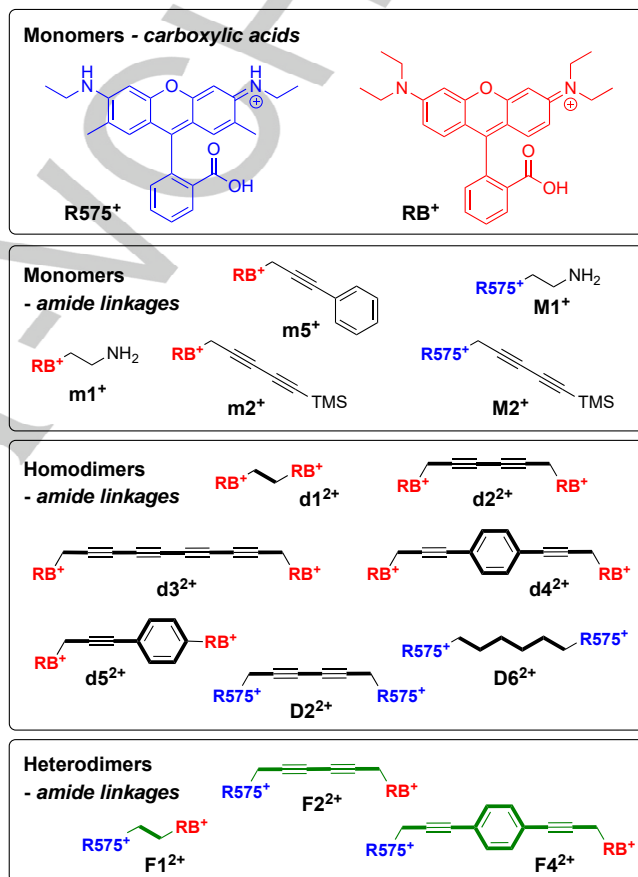


Figure 1. Summary of rhodamine monomers (**m** / **M**), homodimers (**d** / **D**), and heterodimers (**FRET** systems, **F**) subject to studies in this work. For the definition of amide linkages, see Scheme 1.

## Results and Discussion

First we present results from the synthesis part, followed by those from gas-phase ion fluorescence spectroscopy. Finally, we provide an overall discussion based on computed geometric structures of simple model dimers.

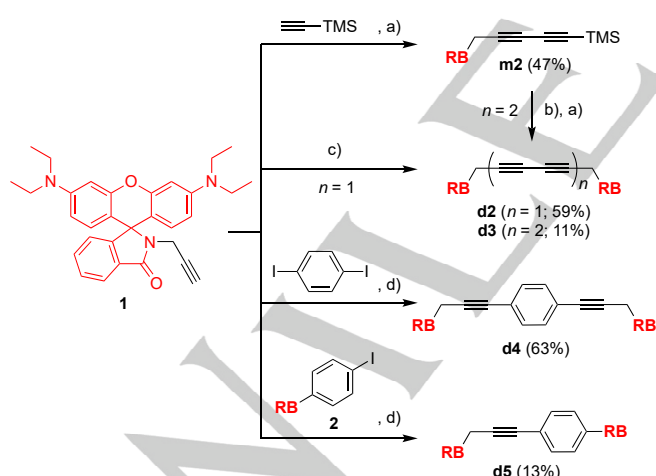
### Synthesis

Rhodamine B dimers **d2-5** were made starting from the monomer **1** according to Scheme 2. The known starting material **1** was made in analogy with a general literature procedure<sup>[5]</sup>, by converting **R575** perchlorate to its acid chloride (using thionyl chloride) that was then treated with propargylamine (see Supporting Information; SI; yields of 65-73%). It has previously been made from the acid chloride generated using POCl<sub>3</sub><sup>[11]</sup> or by using *O*-benzotriazole-*N,N,N',N'*-tetramethyl-uronium hexafluorophosphate (HBTU) and triethylamine to attach propargylamine.<sup>[12]</sup> The other starting material **2** was prepared by treating the acid chloride generated from **RB** chloride with *p*-iodoaniline (yield of 52%); compound **2** has previously been made with the use of toluenesulfonylchloride and DMAP.<sup>[13]</sup> An oxidative coupling of **m4** and trimethylsilylacetylene under Hay conditions (CuCl, TMEDA, and air) gave **m2** in a yield of 26%, while by using Pd(PPh<sub>3</sub>)<sub>2</sub>Cl<sub>2</sub> and CuI an improved yield of 47% was obtained.

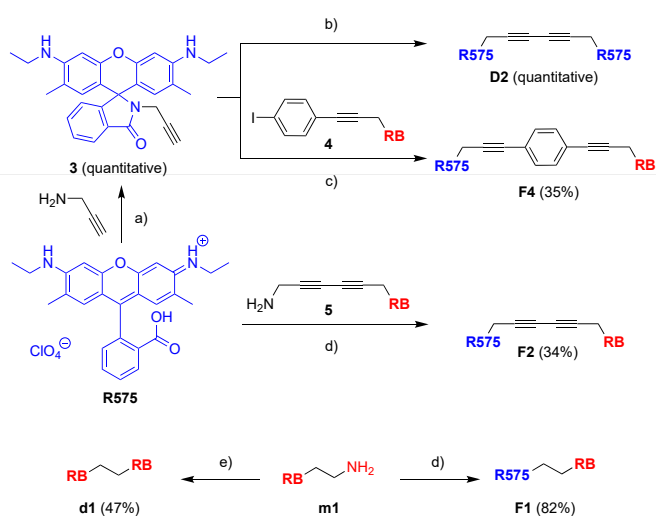
Monomers **m2** and **m4** were now explored as precursors for the homodimers **d2** and **d3**. An oxidative dimerization of **m4**,

## RESEARCH ARTICLE

using conditions of Haley and co-workers<sup>[14]</sup> gave the dimer **d2** in good yield. We note that using these conditions for a heterocoupling between **m4** and trimethylsilylacetylene only gave **m2** in a yield of 4%. Desilylation of **m2** using  $K_2CO_3$  in MeOH followed by an oxidative homocoupling gave **d3** in a yield of 11%. The dimers **d4** and **d5** (as well as monomer **m3**<sup>[11c]</sup> and **m6**) were synthesized by Sonogashira coupling reactions. It was found that this reaction works well when performed in a 1:1 mixture of THF and  $Et_3N$ , with the catalyst system of  $Pd(PPh_3)_2Cl_2$  and CuI. Another specification was that the reaction was done under sonication at 30 °C, which allowed for fairly short reaction times (and previously shown advantageously for Sonogashira couplings<sup>[15]</sup>). Using these conditions and the coupling partners 1,4-diiodobenzene and **m5**, the dimers **d4** and **d5** were obtained in yields of 63% and 13%, respectively.



**Scheme 2.** Synthesis of RB homodimers (lactam forms): a)  $Pd(PPh_3)_2Cl_2$ , CuI,  $Et_3N/PhMe$ , air, rt. b)  $K_2CO_3$ , MeOH/THF; c)  $Pd_2dba_3$ , dppe, CuI,  $I_2$ , DIPA/THF, air, rt. d)  $Pd(PPh_3)_2Cl_2$ , CuI,  $Et_3N/THF$ , 30 °C, )))



**Scheme 3.** Synthesis of **R575** homodimers (lactam forms) and **R575/RB** heterodimers (lactam forms). a) *i.*  $SOCl_2$ ,  $CH_2Cl_2$ ,  $\Delta$ , 2h, *ii.*  $Et_3N$ , MeCN, 0 °C. b)  $Pd_2dba_3$ , dppe, CuI,  $I_2$ , DIPA/THF, air, rt. c)  $Pd(PPh_3)_2Cl_2$ , CuI,  $Et_3N/THF$ , 30 °C, ))) d) *i.* **R575** perchlorate,  $SOCl_2$ ,  $\Delta$ ; *ii.*  $Et_3N$ , MeCN, 0 °C. e) *i.* **RB** chloride,  $SOCl_2$ ,  $\Delta$ , *ii.*  $Et_3N$ , MeCN, 0 °C.

Monomer **3** was readily achieved from **R575** perchlorate according to Scheme 3 in quantitative yield, without need for purification. For synthesis of **3**, a much better yield was obtained via the acid chloride route, while using the formerly reported method by refluxing **R575** perchlorate and propargylamine in ethanol gave a yield of 40–68%;<sup>[16]</sup> the advantage of proceeding via the acid chloride is that this method also works for compounds not soluble in ethanol. The dimer **D2** was prepared in quantitative yield by an oxidative coupling of **3** using  $Pd_2dba_3$ , dppe, CuI, and  $I_2$ . Monomer **M2** could under these conditions be obtained in a yield of 37% (from **3** and trimethylsilylacetylene), but changing to the  $Pd(PPh_3)_2Cl_2$  and CuI catalyst system gave a higher yield of 95%.

The heterodimer **F4** was achieved in a Sonogashira coupling between **3** and **4**, with the conditions described earlier, affording the product in 35% yield. It was possible to form **F2** by coupling terminal alkynes **1** and **3**, but homodimers **d2** and **D2** were also formed, and these could in our hands not be separated from **F2**. To circumvent this problem, monomer **5** was first prepared by coupling *N*-Boc-propargylamine with **3**. After Boc-deprotection, the amine **5** was reacted with the acid chloride of **R575**, furnishing the product **F2** in a yield of 34%. The dimers **d1** and **F1** can easily be made from **m1** by treating it with the acid chloride of the rhodamine monomers and  $Et_3N$  in acetonitrile.

### Gas-Phase Fluorescence Studies

To measure dispersed fluorescence spectra of isolated and mass-selected gaseous ions we use the LUNA setup that in a unique way combines an electrospray ion source with a cylindrical Paul trap (fluorescence cell for mass-selected ions) and a light detection part (detailed in [8]). Briefly, ions made by electrospray ionization of samples dissolved in methanol and acetic acid (10:1) were accumulated in an octopole pretrap that was emptied at a repetition frequency of 20 Hz. Ion bunches were transferred to the Paul trap that was filled with helium buffer gas. Following mass selection, ions were irradiated by a nanosecond laser pulse delivered by a 20-Hz pulsed EKSPALA laser (Nd:YAG laser in combination with an optical parametric oscillator (OPO)). The emitted photons were collected and detected with a spectrometer equipped with a CCD camera (Andor Technology). This sequence was repeated 100 times with no emptying of ion trap in between each injection of ion bunches. A background spectrum with no ions in the trap was then recorded to correct for background photons. A notch filter was placed before the entrance to the spectrometer to reduce the number of scattered photons from the excitation pulse. The spectrometer slit width was 1250  $\mu m$ .

Band maxima for all ions are summarized in Table 1, and all spectra are included in the SI. In the following we discuss the spectra in detail.

## RESEARCH ARTICLE

**Table 1.** Summary of emission band maxima from gas-phase studies. All values are in nm (eV).

R575 <sup>+</sup>	M1 <sup>+</sup>	M2 <sup>+</sup>	D2 <sup>2+</sup>	D6 <sup>2+</sup> [a]
508±2 (2.44±0.01)	508±4 (2.44±0.02)	515±3 (2.41±0.01)	519±4 (2.39±0.02)	528±5 (2.35±0.02)
RB <sup>+</sup>	m1 <sup>+</sup>	m2 <sup>+</sup>	m5 <sup>+</sup>	
543±3 (2.28±0.01)	540±3 (2.30±0.01)	551±3 (2.25±0.01)	549±3 (2.26±0.01)	
d1 <sup>2+</sup>	d2 <sup>2+</sup>	d3 <sup>2+</sup>	d4 <sup>2+</sup>	d5 <sup>2+</sup>
557±4 (2.23±0.02)	549±4 (2.26±0.02)	548±3 (2.26±0.01)	548±3 (2.26±0.01)	552±5 (2.25±0.02)
F1 <sup>2+</sup>	F2 <sup>2+</sup>	F4 <sup>2+</sup>		
556±4 (2.23±0.02)	551±5 (2.25±0.02)	516±3 (2.40±0.01)		

[a] Taken from ref. [5].

**R575 monomers and dimers:** Fluorescence spectra of **M1<sup>+</sup>** and **M2<sup>+</sup>** are shown together with that of **R575<sup>+</sup>** in Figure 2a. As reported earlier, replacement of the carboxylic acid group in **R575<sup>+</sup>** with an amide functionality that terminates in a primary amine (**M1<sup>+</sup>**) has no effect.<sup>[5]</sup> However, a clear redshift occurs when the amide substituent contains a diyne unit (**M2<sup>+</sup>**). The diyne is not in conjugation with the amide, and we therefore ascribe the redshift to polarization of the  $\pi$ -electronic cloud in the electric field from the xanthenone cation to give a favorable charge induced-dipole interaction (Figure 3). This interaction increases in strength after photoexcitation of the xanthenone on account of the in general higher polarizability of an excited state than of a ground state<sup>[17]</sup>; the positive charge distribution in the xanthenone moves closer towards the diyne that as a result gets even more polarized.

Now, a homodimer with the diyne bridge (**D2<sup>2+</sup>**) displays a spectrum that is similar to that of **M2<sup>+</sup>** except that it is broadened towards the red (Figure 2b,c). The broadening is likely the result of multiple structures present in the ion cloud, and that each structure is somewhat flexible. It is noteworthy that the band maximum for a homodimer where the bridge contains six methylene units (**D6<sup>2+</sup>**, spectrum included in Figure 2b), *i.e.*, same number of carbon atoms in bridge as in **D2<sup>2+</sup>**, is significantly redshifted. The red end of the two **D2<sup>2+</sup>** and **D6<sup>2+</sup>** spectra is, however, similar. The redshifted emission from **D6<sup>2+</sup>** relative to **R575<sup>+</sup>** was earlier ascribed to a Stark effect as the internal Coulomb repulsion between the two cationic dyes is reduced after photoexcitation<sup>[5]</sup>; again ascribed to the higher polarizability in an excited state. Interestingly, the  $\pi$ -spacer seems to counteract this effect. Indeed, in a simple picture each dye will polarize the  $\pi$ -spacer such that there is an excess of negative charge close to each dye and a positive charge in the center of the spacer (Figure 3). The result is a  $\pi$ -spacer with a quadrupole moment, which provides an electric field at each dye that opposes that from the positive charge. The  $\pi$ -spacer shields one dye from the other, thereby lowering the effect of internal Coulomb repulsion.

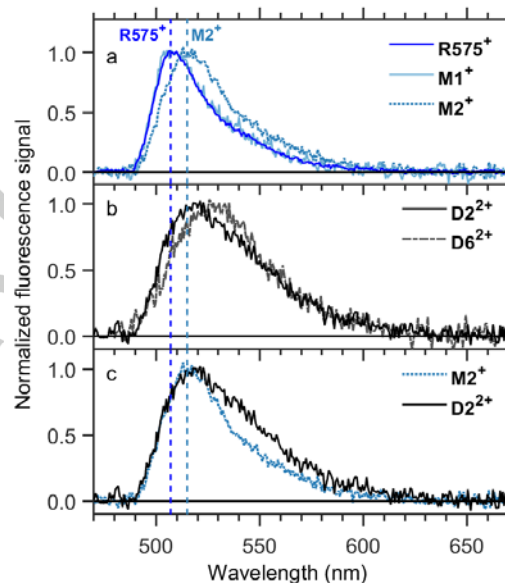


**Figure 2.** Gas-phase fluorescence spectra of (a) R575 monomers and (b) R575 dimers. In (c) spectra of a R575 monomer and the corresponding dimer are presented for comparison. The dashed lines indicate band maxima of **R575<sup>+</sup>** (furthest to the blue) and of **M2<sup>+</sup>** (furthest to the red). All spectra were recorded with an excitation wavelength of 487 nm.

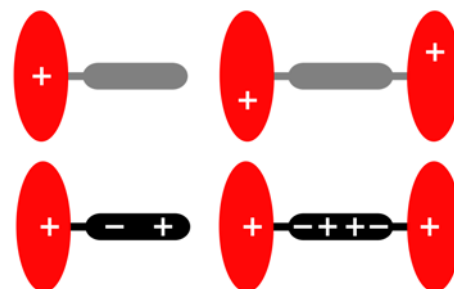


**Figure 3.** Top: Symmetric dye (in red) with one positive charge and a linker (in grey) that is composed of methylene units. The charge is evenly distributed over the dye but is on the figure shown as a point charge in the center. The charge distribution becomes asymmetric when two cationic dyes are tethered together due to the internal Coulomb repulsion and the high polarizability of the dyes. Bottom: A  $\pi$ -linker (in black) is polarized in the field from one cationic dye; the electric field due to the induced dipole moment of the  $\pi$ -linker acts back and changes the charge distribution in the dye, *i.e.*, the positive charge moves on average towards the  $\pi$ -linker. When a second dye is attached, a quadrupole moment is induced in the  $\pi$ -spacer, which effectively shields the two positive charges.

**RB monomers and dimers:** Figure 4 shows spectra of monomers and dimers. A  $\pi$ -electron cloud in the form of a diyne (**m2<sup>+</sup>**) or phenylethynyl (**m5<sup>+</sup>**) causes a significantly redshifted spectrum compared to that of the parent monomer species (**RB<sup>+</sup>**). As before, we ascribe this to a polarization effect. The spectrum of **m1<sup>+</sup>** is slightly to the blue of **RB<sup>+</sup>**, which may be due to some interaction between the xanthenone and the primary amine.

Spectra of homodimers with  $\pi$ -spacers are surprisingly similar to that of monomers that contain a  $\pi$ -appendage. There is little dependence on the  $\pi$ -spacer; the spectra of **d2<sup>2+</sup>** (diyne), **d3<sup>2+</sup>** (tetrayne), and **d4<sup>2+</sup>** (diethynylbenzene unit) are almost identical while that of **d5<sup>2+</sup>** (phenylethynyl) is slightly broadened to

## RESEARCH ARTICLE

the red. In contrast, the spectrum of  $\mathbf{d1}^{2+}$  where two methylene units bridge the two fluorophores is significantly redshifted as earlier reported also for homodimers of  $\mathbf{R575}^+$ .<sup>[5]</sup> Taken together, these results indicate that a  $\pi$ -spacer shields the two positive charges in homodimers, and therefore that the spacer length is of less importance than is the case for methylene units (Figure 3).

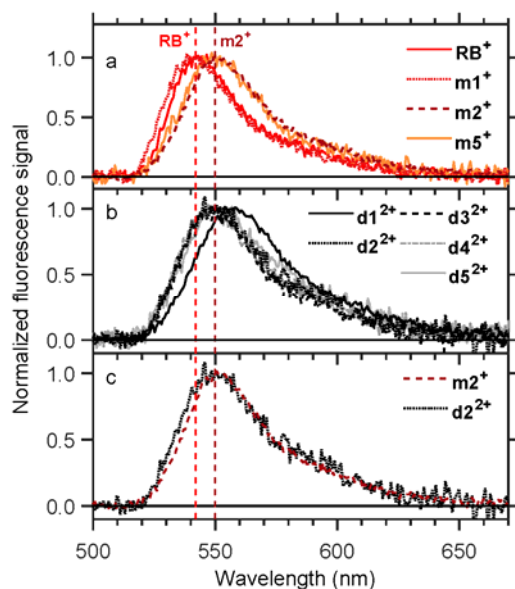


**Figure 4.** Gas-phase fluorescence spectra of (a) RB monomers and (b) RB dimers. Spectra of a RB monomer and the corresponding dimer are shown in (c) for comparison. The dashed lines indicate absorption band maxima of  $\mathbf{RB}^+$  (furthest to the blue) and of  $\mathbf{m2}^+$  (furthest to the red). All spectra were recorded with an excitation wavelength of 513 nm.

**Heterodimers:** Our work includes three heterodimers with the  $\mathbf{R575}^+/\mathbf{RB}^+$  FRET pair. In the first ( $\mathbf{F1}^{2+}$ ) the two dyes are bridged by two methylene groups. Two spectra obtained after photoexcitation at either 487 nm or 513 nm are shown in Figure 5. Except for a small shoulder to the blue (515 – 525 nm) for 487-nm excitation, the spectra are quite similar. It should be noted, however, that the notch filter for 513-nm excitation prevents the transmission of photons to the spectrometer in a small region around 513 nm ( $514 \pm 9$  nm). In any case, fluorescence occurs dominantly from the  $\mathbf{RB}^+$  dye, either due to direct excitation of the dye in the heterodimer or after FRET. The emission spectrum is significantly redshifted compared to that of  $\mathbf{RB}^+$  monomers and is almost identical to that of  $\mathbf{d1}^{2+}$  ( $\mathbf{RB}^+$  homodimer with two methylene units). As discussed above and in previous work on a heterodimer of  $\mathbf{R575}^+$  and  $\mathbf{R640}^+$ ,<sup>[6]</sup> this is simply due to the electric field that one cationic dye senses from the other. The fact that the spectra of  $\mathbf{F1}^{2+}$  and  $\mathbf{d1}^{2+}$  are nearly identical excludes the possibility of exciton coupling as the energy of an exciton state formed from a linear combination of two  $\mathbf{RB}^+$  excited states is clearly different to that from a linear combination of  $\mathbf{R575}^+$  and  $\mathbf{RB}^+$  excited states. Also, even though the alkyl spacer is small, the separation between the two xanthenes is too large (11 Å or more, *vide infra*) for exciton coupling really to be significant. The small shoulder towards the blue observed in the 487-nm excitation spectrum of  $\mathbf{F1}^{2+}$  is indicative of some minor emission from  $\mathbf{R575}^+$ . This may originate from structures where the relative dipole orientation factor is small, which results in short Förster

distances and less efficient energy transfer; we will return to possible geometries later on.

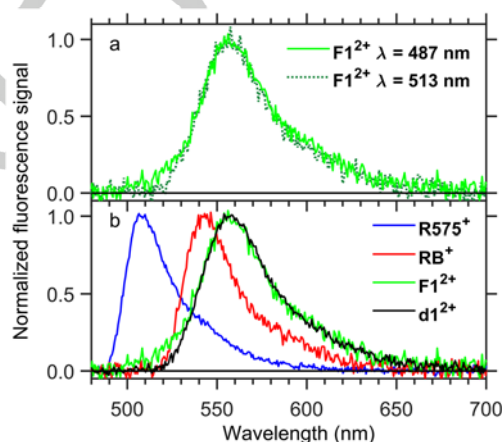


**Figure 5.** Gas-phase fluorescence spectra of (a)  $\mathbf{F1}^{2+}$  recorded using two different excitation wavelengths (487 nm and 513 nm). The 487-nm spectrum is also presented in (b) together with those of  $\mathbf{R575}^+$  and  $\mathbf{RB}^+$  dye monomers (487-nm and 513-nm excitation, respectively) and a  $\mathbf{d1}^{2+}$  RB dimer (513-nm excitation).

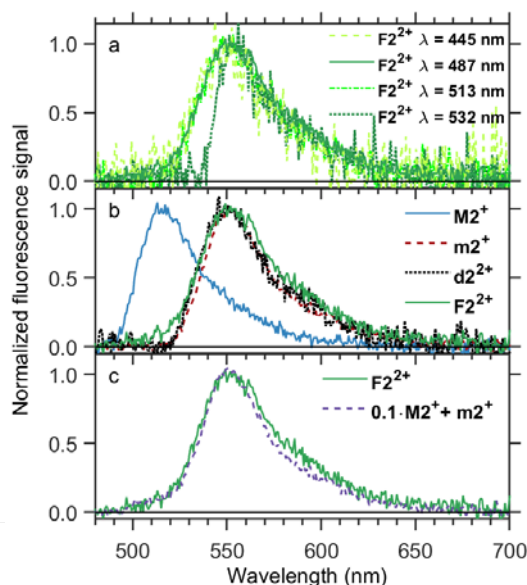


**Figure 6.** Gas-phase fluorescence spectra of (a)  $\mathbf{F2}^{2+}$  recorded using four different excitation wavelengths (445 nm, 487 nm, 513 nm, and 532 nm). The hole in the 532-nm spectrum is due to blocking by the notch filter ( $533 \pm 9$  nm). The 487-nm spectrum is also presented in (b) together with those of  $\mathbf{M2}^+$  and  $\mathbf{m2}^+$  dye monomers (487-nm and 513-nm excitation, respectively) and the  $\mathbf{d2}^{2+}$  RB dimer (513 nm). A sum of the  $\mathbf{m2}^+$  spectrum and 0.1 times the  $\mathbf{M2}^+$  spectrum is shown in (c) together with the  $\mathbf{F2}^{2+}$  spectrum.

In heterodimer  $\mathbf{F2}^{2+}$ , the two dyes are bridged by a spacer that contains a diyne. Spectra recorded at excitation wavelengths of 445 nm, 487 nm, 513 nm, and 532 nm are shown in Figure 6a. At higher wavelengths, the  $\mathbf{RB}^+$  absorption increases relative to that of  $\mathbf{R575}^+$ . The notch filter prevents emitted photons in a region around the excitation wavelength to be transmitted to the

## RESEARCH ARTICLE

spectrometer, which implies that only the part of the spectrum 9 nm above the excitation wavelength is valid for 513 nm and 532 nm. However, as no dependence on excitation wavelength is seen, we conclude that any structural change before FRET is limited. Indeed, if excitation of **R575<sup>+</sup>** had led to a geometry change of the dimer, we would expect a Stokes shift for the emission from **RB<sup>+</sup>** after FRET.

From Figure 6b, it is clearly evident that the emission spectrum of **RB<sup>+</sup>** in **F2<sup>2+</sup>** is the same as those of **m2<sup>+</sup>** (monomer **RB<sup>+</sup>** with diyne linkage) and **d2<sup>2+</sup>** (homodimer of **RB<sup>+</sup>** with diyne  $\pi$ -spacer). The spectrum of **R575<sup>+</sup>** monomers with diyne linkage (**M2<sup>+</sup>**) is also included in the figure for comparison. Indeed, a linear combination of the **M2<sup>+</sup>** (10%) and **m2<sup>+</sup>** (100%) normalized monomer spectra can reasonably well reproduce the spectrum of **F2<sup>2+</sup>**. To obtain a FRET efficiency we need to consider the absorption cross sections of the two dyes as well as the internal conversion rates.

Gas-phase absorption spectra of **RB<sup>+</sup>** and **R575<sup>+</sup>** parent species were earlier reported by Jockusch and co-workers.<sup>[18]</sup> The absorption by **RB<sup>+</sup>** at 487 nm is about 30% that at maximum absorption at 531 nm. In the case of **R575<sup>+</sup>**, the maximum absorption is at 495 nm, and at 487 nm the absorption is about 95%. Assuming equal absorption cross sections, the absorption by **R575<sup>+</sup>** is about three times larger than that by **RB<sup>+</sup>** at 487 nm. This assumption is somewhat justified from similar fluorescence signals from the two monomer dyes when they are photoexcited close to their maximum absorption. In the heterodimer both dyes have about 10 nm redshifted emission compared to **R575<sup>+</sup>** and **RB<sup>+</sup>** parent monomers. If we assume the absorption spectra are also redshifted by 10 nm, the absorption by **R575<sup>+</sup>** is about five times larger than by **RB<sup>+</sup>** in the heterodimer. The internal conversion rates of both dyes are likely low as the dyes are both strongly fluorescent. If we assume them to be equal for **R575<sup>+</sup>** and **RB<sup>+</sup>** in the heterodimer, we estimate based on the absorption cross sections and the **F2<sup>2+</sup>** spectrum, a FRET efficiency of about 89%.

Finally, spectra of the third heterodimer, **F4<sup>2+</sup>** (diethynylbenzene spacer unit), recorded with three different excitation wavelengths are shown in Figure 7a. Again, the spectra look similar at the red end, and we conclude that the fluorescence from **RB<sup>+</sup>** is independent of whether the excited state is formed after direct photon absorption or after FRET, indicative of no or limited geometry change when **R575<sup>+</sup>** is initially photoexcited. The most striking result for **F4<sup>2+</sup>** is that emission occurs dominantly from **R575<sup>+</sup>**. Panel b in the figure reveals that the emission band maximum is the same as that of **M2<sup>+</sup>** (**R575<sup>+</sup>** with diyne), again demonstrating that the charge from another dye has little effect in the presence of a  $\pi$ -spacer. The panel also includes the **m5<sup>+</sup>** (**RB<sup>+</sup>** with phenylethynyl) spectrum. A linear combination of the two model monomer spectra ( $0.25 \cdot m5^+ + M2^+$ ) are seen in panel c to fully reproduce the **F4<sup>2+</sup>** spectrum. After correction for the absorption of 487-nm photons directly by **RB<sup>+</sup>** in the heterodimer, we estimate the FRET efficiency to be only about 4%.

The RET seen for **F4<sup>2+</sup>** is surprisingly small considering the short interfluorophore separation (23 Å, *vide infra*), which indicates that Through Bond Energy Transfer (TBET) is not active. TBET normally accounts for faster RET than predicted by FRET and occurs via a  $\pi$ -linker (see e.g. a discussion of TBET in [10a]). However, a CH<sub>2</sub> group at each end of the linker in **F4<sup>2+</sup>** breaks the direct conjugation with the dye; i.e., hyperconjugation is necessary to mediate  $\pi$ -orbital overlap.

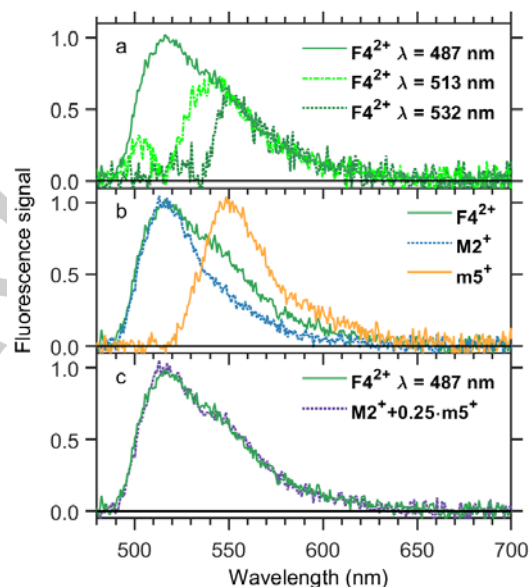


**Figure 7.** Gas-phase fluorescence spectra of (a) **F4<sup>2+</sup>** recorded using three different excitation wavelengths (487 nm, 513 nm, and 532 nm). Two of the excitation wavelengths (513 nm, 532 nm) are within the fluorescence band. The holes in the spectra are due to blocking by the notch filter. The 487-nm spectrum is also presented in (b) together with those of **M2<sup>+</sup>** and **m5<sup>+</sup>** dye monomers (487-nm and 513-nm excitation, respectively). A sum of the **M2<sup>+</sup>** spectrum and 0.25 times the **m5<sup>+</sup>** spectrum is shown in (c) together with the **F4<sup>2+</sup>** spectrum.

### Computational Studies

To explore structural heterogeneity, we have done density functional theory (DFT) calculations on a simple model homodimer (Figure 8, top) using the Gaussian program package<sup>[19]</sup>. We chose the rhodamine core structure and two methylene units as bridge to limit the computational time. Seven different geometries were found by optimization at the B3LYP/6-31G level and are shown in Figure 8; there are of course more possible conformers but we believe that those obtained serve as good representatives. Also vibrational frequencies were calculated to verify that all structures are local minima and not transition states. Based on the frequencies the internal energy is estimated to 0.7 eV at 298 K. The structures were subjected to single-point calculations at the B3LYP/6-311++G(2d,p) (SCF=Tight) level. The highest-energy isomer (**VII**) is 0.55 eV higher in energy than the lowest-energy one (**I**).

A summary of relative energies, distances between the fluorophore centers ( $R$ ), and relative dipole orientation factors ( $\kappa^2$ ) are given in Table 2 (coordinates and details on how to calculate  $\kappa^2$  are given in the SI). The interfluorophore distance varies between 11.0 Å (conformer **II**) and 12.7 Å (**III**). The lowest value of  $\kappa^2$  is 0.04 (**V**) and the highest 0.95 (**I**). Indeed, the two lowest-energy structures have significantly different  $\kappa^2$  values (0.95 and 0.16) and  $R$ -values (12.5 Å and 11.0 Å). These two structures will give different fluorescence spectra as the charge-induced polarization of the two fluorophores is different, which accounts for broader spectra seen for dimers than for monomers. Only Stark-shifted emission is seen for dimers as the monomers only carry one positive charge. In addition, the higher-energy structures will contribute to this broadening, in particular if equilibrium is not established under the experimental conditions. While the ions undergo thermalizing collisions with the room-temperature helium-buffer gas in the trap, some RF-heating is

## RESEARCH ARTICLE

unavoidable (due to energetic collisions between high-velocity ions and helium). The large variation in  $\kappa^2$  also suggests that structures are present for which FRET is less likely to occur even though  $R$  is short. These could explain the small emission seen from **R575\*** after photoexcitation of **F12\*** (Figure 5).

Calculated structures of homodimers modeling **d2<sup>2+</sup>** / **D2<sup>2+</sup>** / **F2<sup>2+</sup>** and **d4<sup>2+</sup>** / **F4<sup>2+</sup>** are shown in Figure 9, again using the simplified rhodamine core structure for each dye; results are summarized in Table 3. Here the linear, rigid  $\pi$ -linker limits the number of possible structures. For **F2<sup>2+</sup>** models, we found three structures extremely close in energy (basically isoenergetic), and where the two dyes are oriented with nearly parallel or perpendicular transition dipole moments providing high and low  $\kappa^2$  values, respectively (Table 3 and Figure 9). The former orientation favors FRET in contrast to the latter. In the case of **F4<sup>2+</sup>** models, we locate two low-lying structures that both have nearly parallel transition dipole moments (Table 3 and Figure 9). A low-lying transition state connects these “anti” (I’) and “syn” (II’’) structures from a rotation around the  $\pi$ -spacer-(CH<sub>2</sub>) single bond. The transition state is 0.014 eV higher in energy than the “anti” form, and at room temperature there is therefore basically free rotation around the single bond. Importantly, the structures found close in energy for **F2<sup>2+</sup>** and **F4<sup>2+</sup>** models and the low-lying transition state for the **F4<sup>2+</sup>** model indicate that the two dyes to a good approximation can rotate freely relative to each other, along an almost linear rod, within the excited-state lifetime, and therefore that a value of 2/3 is a reasonable estimate for  $\kappa^2$  for both heterodimers. Likewise, Winters *et al.*<sup>[20]</sup> found based on DFT calculations that the ground state of a butadiyne-linked porphyrin dimer has a broad distribution of dihedral angles at room temperature due to a very low barrier for rotation.

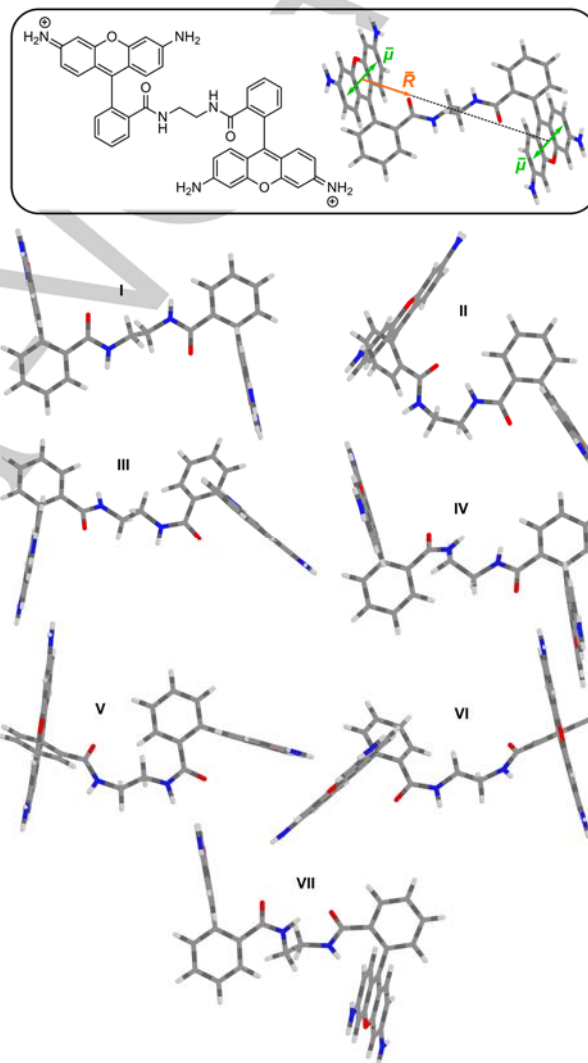


**Figure 8.** Optimized geometries of the simplified dimer structure shown on top. The transition dipole moments and the interfluorophore distance vector are indicated for I (top).

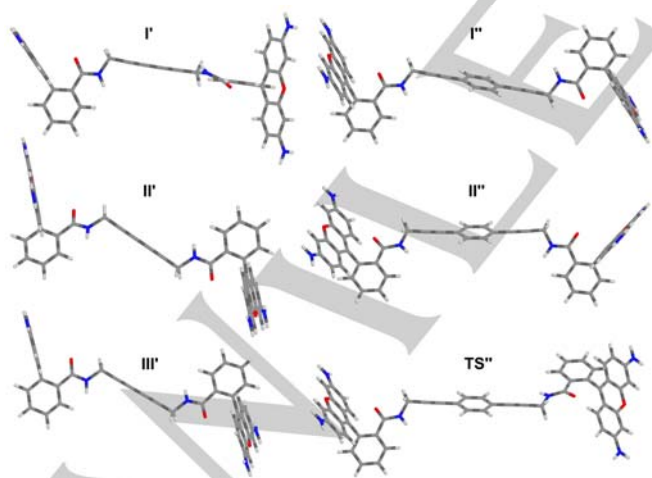
**Table 2.** Relative conformer energies, interfluorophore distances ( $R$ ), and relative dipole orientation factors ( $\kappa^2$ ) for homodimers shown in Figure 8.

Conformer	$E$ (in eV)	$R$ (in Å)	$\kappa^2$
I	0	12.5	0.95
II	0.049	11.0	0.16
III	0.33	12.7	0.50
IV	0.33	12.3	0.84
V	0.35	11.4	0.04
VI	0.40	11.9	0.17
VII	0.55	11.2	0.49

## RESEARCH ARTICLE

**Table 3.** Relative conformer energies, interfluorophore distances ( $R$ ), and relative dipole orientation factors ( $\kappa^2$ ) for acetylenic scaffolds shown in Figure 9.

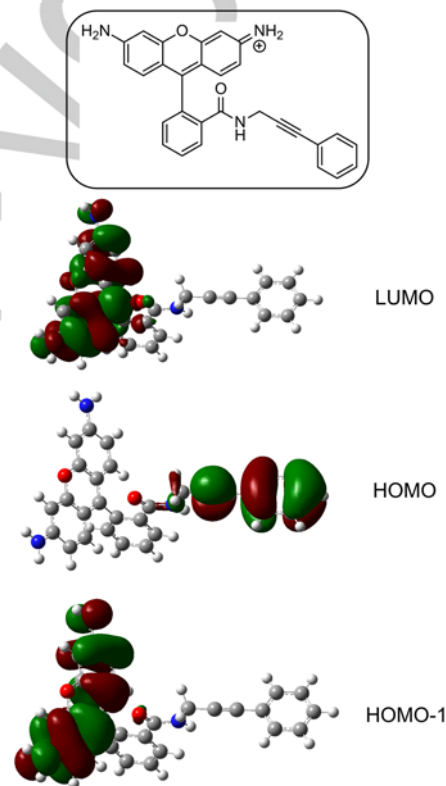
Conformer	$E$ (in eV)	$R$ (in Å)	$\kappa^2$
I'	0	18.4	0.008
II'	0.0066	18.1	0.85
III'	0.012	18.2	0.91
I''	0	22.6	0.95
II''	0.0014	22.7	0.79
TS''	0.014	22.7	0.061

**Figure 9.** Optimized geometries of simplified dimers with acetylenic bridges; same rhodamine units as those shown in Figure 8, top. Left: Butadiyn bridge. Right: Diethynylbenzene bridge.

Based on the assumption of  $\kappa^2$  being 2/3 for both  $\mathbf{F2}^{2+}$  and  $\mathbf{F4}^{2+}$ , we can provide an estimate of the Förster distance simply from calculated interfluorophore distances. In  $\mathbf{F2}^{2+}$  the energy-transfer efficiency is more than 50%, which implies that  $R(\mathbf{F2}^{2+}) < R_0$  while in  $\mathbf{F4}^{2+}$  the efficiency is less than 50% and  $R(\mathbf{F4}^{2+}) > R_0$ . As  $R(\mathbf{F2}^{2+}) = 18 \text{ Å}$  and  $R(\mathbf{F4}^{2+}) = 23 \text{ Å}$ , an estimate for  $R_0$  midway between the two  $R$  values is  $20.5 \pm 2.5 \text{ Å}$ . This value is significantly less than that of  $67 \text{ Å}$  reported by Jockusch and co-workers<sup>[21]</sup> for the  $\mathbf{R575}^+/\mathbf{R640}^+$  FRET pair tethered to a peptide, even though the spectral overlap is larger for  $\mathbf{R575}^+/\mathbf{RB}^+$  than for  $\mathbf{R575}^+/\mathbf{R640}^+$ . We note that  $R_0^6$  is proportional to the spectral overlap and to  $\kappa^2$ , and that  $\kappa^2$  was assumed to be 2/3 for the  $\mathbf{R575}^+/\mathbf{R640}^+$  FRET pair. This significant difference in  $R_0$  reflects the efficient screening provided by a  $\pi$ -spacer as such screening lowers the dipole-dipole interaction between the two dyes and as a result the Förster distance.

Finally, we calculated the molecular orbitals of the rhodamine model with a phenylethynyl appendage at the MP2/6-311++G(2d,p) // B3LYP/6-31G level of theory (Figure 10). It is evident that the HOMO is located on the phenylethynyl unit with no overlap with the xantheno dye. Likewise, the HOMO-1 and the LUMO are on the xantheno dye, and there is no  $\pi$ -orbital overlap

with the phenylethynyl unit. This picture supports our assumption from earlier that the energy transfer is not mediated by the  $\pi$ -spacer in heterodimers.

**Figure 10.** Model rhodamine with ethynylphenyl appendage (structure shown in box). MP2/6-311++G(2d,p) // B3LYP/6-31G calculated orbitals of HOMO-1, HOMO, and LUMO.

It is worth to mention that while a polarity model does provide a simple explanation for our results, the molecules with alkyl spacers have rather complex structures (Figure 8) rendering a direct comparison of linkers somewhat difficult. Indeed, as our calculations show, an alkyl spacer allows for more conformational freedom. In contrast, the molecules with  $\pi$ -spacers are nearly linear (Figure 9), which is optimum for polarization of the  $\pi$ -electrons in the triple bonds. For comparison, buta-1,3-diyne has a slightly larger boiling point than butane, which is partly ascribed to the polarization of the  $\pi$ -electrons in the former molecule and as a result greater dispersion forces. It would be interesting to better establish the connection between geometric structure and Stark-shifted emission. This would require conformer selection, for example done by ion-mobility spectrometry. Another approach would be cold-ion spectroscopy. At low temperatures, it is possible to address each conformer selectively due to specific absorption lines. Our instrumental work is going in this direction with the current construction of LUNA2, a setup operating at 77 K, and hopefully also a cryogenically cooled setup in a foreseeable future.

## Conclusion

## RESEARCH ARTICLE

In this work, we have reported the synthesis of new dyads where two charged dyes (Rhodamine 575 or Rhodamine B) are bridged by almost linear linkers (rods). The preparations were based on acetylenic coupling reactions, and oxidative alkyne-alkyne dimerizations were finely tuned to reach optimum conditions for the various rhodamine scaffolds.

Gas-phase fluorescence studies on the cationic dyes reveal strong polarization of the  $\pi$ -linker when it experiences the electric field from one or two dyes. As a result,  $\pi$ -spacers provide efficient shielding of charges, *i.e.*, they reduce the Coulomb interaction between two dye cations. This was evidenced from almost identical fluorescence spectra of homodimers and corresponding monomer derivatives. In contrast, two dye cations repel each other strongly when connected by an alkyl bridge, which results in red-shifted emission spectra due to the Stark effect.

In the case of heterodimers, a  $\pi$ -spacer acts as a shield against the dipole-dipole interaction that governs energy transfer from donor to acceptor. Hence the energy-transfer efficiency is much reduced compared to that for corresponding systems with alkyl spacers. Indeed, from DFT-calculated structures, we provide an estimated Förster distance of only  $20.5 \pm 2.5$  Å for the Rhodamine 575 / Rhodamine B FRET pair tethered together with a  $\pi$ -spacer despite a high spectral overlap of donor emission and acceptor absorption. This screening effect may have direct implications on the energy transfer when fluorophores are integrated in biological systems where aromatic units potentially could act as  $\pi$ -shields.

## Acknowledgements

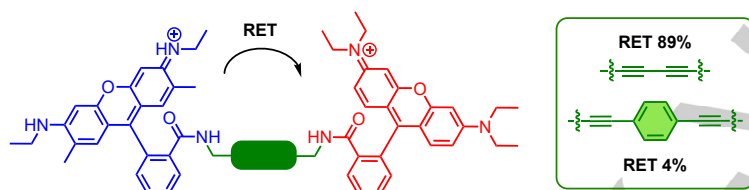
SBN and MBN acknowledge support from the Independent Research Fund Denmark | Natural Sciences (9040-00041B).

**Keywords:** Alkynes • Dyads • Cross-coupling • Fluorescence • gas-phase FRET

- [1] Y. C. Cheng, G. R. Fleming, *Annu. Rev. Phys. Chem.* **2009**, *60*, 241-262.
- [2] C. T. Middleton, K. de la Harpe, C. Su, Y. K. Law, C. E. Crespo-Hernandez, B. Kohler, *Annu. Rev. Phys. Chem.* **2009**, *60*, 217-239.
- [3] C. R. Cantor, P. R. Schimmel, *Biophysical Chemistry, Part II, Techniques for the Study of Biological Structure and Function*, W. H. Freeman and Company, New York, **1980**, p. 392f.
- [4] J. R. Lakowicz, *Principles of Fluorescence Spectroscopy*, 2nd edn, Kluwer Academic/Plenum Publishers, New York, **1999**.
- [5] C. Kjær, H. Lissau, N. K. G. Salinas, A. Ø. Madsen, M. H. Stockett, F. E. Storm, T. H. Hansen, J. U. Andersen, B. W. Laursen, K. V. Mikkelsen, M. Brøndsted Nielsen, S. Brøndsted Nielsen, *ChemPhysChem* **2019**, *20*, 533-537.
- [6] C. Kjær, Y. Zhao, M. H. Stockett, L. Chen, K. Hansen, S. Brøndsted Nielsen, *Phys. Chem. Chem. Phys.* **2020**, *22*, 11095-111000.
- [7] a) J. T. Khoury, S. E. Rodriguez-Cruz, J. H. Parks, *J. Am. Soc. Mass Spectrom.* **2002**, *13*, 696-708; b) V. Frankevich, X. W. Guan, M. Dashtiev, R. Zenobi, *Eur. J. Mass Spectrom.* **2005**, *11*, 475-482; c) Q.-Z. Bian, M. W. Forbes, F. O. Talbot, R. A. Jockusch, *Phys. Chem. Chem. Phys.* **2010**, *12*, 2590-2598; d) M. Kordel, S. Schooss, C. Neiss, L. Walter, M. M. Kappes, *J. Phys. Chem. A* **2010**, *114*, 5509-5514; e) K. Honma, *Phys. Chem. Chem. Phys.* **2018**, *20*, 26859-26869.
- [8] a) M. H. Stockett, J. Houmøller, K. Støchkel, A. Svendsen, S. Brøndsted Nielsen, *Rev. Sci. Instrum.* **2016**, *87*, 053103; b) M. H. Stockett, J. Houmøller, S. Brøndsted Nielsen, *J. Chem. Phys.* **2016**, *145*, 104303.
- [9] a) S. M. J. Wellman, R. A. Jockusch, *J. Phys. Chem. A* **2015**, *119*, 6333-6338; b) J. A. Wyer in *Photophysics of Ionic Biochromophores* (Eds.: J. A. Wyer, S. Brøndsted Nielsen), Springer, Berlin/Heidelberg, **2003**, Chapter 3.
- [10] a) B. Albinsson, M. P. Eng, K. Pettersson, M. U. Winters, *Phys. Chem. Chem. Phys.* **2007**, *9*, 5847-5864; b) P. P. Lainé, S. Campagna, F. Loiseau, *Coord. Chem. Rev.* **2008**, *252*, 2552-2571; c) M. Natali, S. Campagna, F. Scandola, *Chem. Soc. Rev.* **2014**, *43*, 4005-4018; d) Y. Hou, X. Zhang, K. Chen, D. Liu, Z. Wang, Q. Liu, J. Zhao, A. Barbon, *J. Mater. Chem. C* **2019**, *7*, 12048-12074.
- [11] a) M. J. Jou, X. Chen, K. M. K. Swamy, H. N. Kim, H.-J. Kim, S. Lee, J. Yoon, *Chem. Commun.* **2009**, *46*, 7218-7220; b) O. A. Egorova, H. Seo, A. Chatterjee, K. H. Ahn, *Org. Lett.* **2010**, *12*, 401-403; c) X. Cao, W. Lin, Y. Ding, *Chem. Eur. J.* **2011**, *17*, 9066-9069.
- [12] a) N. B. Yapici, S. Jockusch, A. Moscatelli, S. R. Mandalapu, Y. Itagaki, D. K. Bates, S. Wiseman, K. M. Gibson, N. J. Turro, L. Bi, *Org. Lett.* **2012**, *14*, 50-53; b) N. B. Yapici, S. R. Mandalapu, T.-L. Chew, S. Khuon, L. Bi, *Bioorg. Med. Chem. Lett.* **2012**, *22*, 2440-2443; c) N. B. Yapici, Y. Bi, P. Li, X. Chen, X. Yan, S. R. Mandalapu, M. Faucett, S. Jockusch, J. Ju, K. M. Gibson, W. J. Pavan, L. Bi, *Sci. Rep.* **2015**, *5*, 8576.
- [13] M. K. Lee, P. Rai, J. Williams, R. J. Twieg, W. E. Moerner, *J. Am. Chem. Soc.* **2014**, *136*, 14003-14006.
- [14] E. L. Spitler, J. M. Monson, M. M. Haley, *J. Org. Chem.* **2008**, *73*, 2211-2223.
- [15] a) K. Qvortrup, A. S. Andersson, J.-P. Mayer, A. S. Jepsen, M. Brøndsted Nielsen, *Synlett* **2004**, 2818-2820; b) A. S. Andersson, K. Qvortrup, E. R. Torbensen, J.-P. Mayer, J.-P. Gisselbrecht, C. Boudon, M. Gross, A. Kadziola, K. Kilså, M. Brøndsted Nielsen, *Eur. J. Org. Chem.* **2005**, 3660-3671; c) A. R. Gholap, K. Venkatasana, R. Pasricha, T. Daniel, R. J. Lahoti, K. V. Srinivasan, *J. Org. Chem.* **2005**, *70*, 4869-4872; d) S. S. Palimkar, P. H. Kumar, R. L. Lahoti, K. V. Srinivasan, *Tetrahedron* **2006**, *62*, 5109-5115; e) N. Fu, Y. Zhang, D. Yang, B. Chen, X. Wu, *Catalysis Comm.* **2008**, *9*, 976-979.
- [16] a) W. Lin, X. Cao, Y. Ding, L. Yuan, L. Long, *Chem. Commun.* **2010**, *46*, 3529-3531; b) R. Kagit, M. Yildirim, O. Ozay, S. Yesilot, H. Ozay, *Inorg. Chem.* **2014**, *53*, 2144-2151; c) J.-T. Hou, K. Li, K.-K. Yu, M.-Z. Ao, X. Wang, X.-Q. Yu, *Analyst* **2013**, *138*, 6632-6638.
- [17] P. Suppan, N. Ghoneim, *Solvatochromism*, The Royal Society of Chemistry, Cambridge, UK, **1997**, Chapter 3.
- [18] a) M. W. Forbes, R. A. Jockusch, *J. Am. Soc. Mass Spectrom.* **2011**, *22*, 93-109; b) S. K. Sagoo, R. A. Jockusch, *J. Photochem. Photobiol. A: Chem.* **2011**, *220*, 173-178.
- [19] Gaussian 03, Revision D.01, M. J. Frisch, G. W. Trucks, H. B. Schlegel, G. E. Scuseria, M. A. Robb, J. R. Cheeseman, J. A. Montgomery, Jr., T. Vreven, K. N. Kudin, J. C. Burant, J. M. Millam, S. S. Iyengar, J. Tomasi, V. Barone, B. Mennucci, M. Cossi, G. Scalmani, N. Rega, G. A. Petersson, H. Nakatsuji, M. Hada, M. Ehara, K. Toyota, R. Fukuda, J. Hasegawa, M. Ishida, T. Nakajima, Y. Honda, O. Kitao, H. Nakai, M. Klene, X. Li, J. E. Knox, H. P. Hratchian, J. B. Cross, V. Bakken, C. Adamo, J. Jaramillo, R. Gomperts, R. E. Stratmann, O. Yazyev, A. J. Austin, R. Cammi, C. Pomelli, J. W. Ochterski, P. Y. Ayala, K. Morokuma, G. A. Voth, P. Salvador, J. J. Dannenberg, V. G. Zakrzewski, S. Dapprich, A. D. Daniels, M. C. Strain, O. Farkas, D. K. Malick, A. D. Rabuck, K. Raghavachari, J. B. Foresman, J. V. Ortiz, Q. Cui, A. G. Baboul, S. Clifford, J. Cioslowski, B. B. Stefanov, G. Liu, A. Liashenko, P. Piskorz, I. Komaromi, R. L. Martin, D. J. Fox, T. Keith, M. A. Al-Laham, C. Y. Peng, A. Nanayakkara, M. Challacombe, P. M. W. Gill, B. Johnson, W. Chen, M. W. Wong, C. Gonzalez, J. A. Pople, Gaussian, Inc., Wallingford CT, 2004.
- [20] M. U. Winters, J. Kärnbratt, M. Eng, C. J. Wilson, H. L. Anderson, B. Albinsson, *J. Phys. Chem. C* **2007**, *111*, 7192-7199.
- [21] F. O. Talbot, A. Rullo, H. Yao, R. A. Jockusch, *J. Am. Chem. Soc.* **2010**, *132*, 16156-16164.

## RESEARCH ARTICLE

## Entry for the Table of Contents



**A communication barrier:** A  $\pi$ -spacer blocks the electronic communication between two ionic rhodamine dyes in a dyad isolated *in vacuo* as it screens for the electric field that each dye senses from the other. As a result energy transfer based on the dipole-dipole interaction is less efficient than that for systems with alkyl spacers. This conclusion is reached from gas-phase ion fluorescence spectroscopy of monomers and dimers prepared by acetylenic coupling reactions.

Institute and/or researcher Twitter usernames: Mogens Brøndsted @mogens\_br